



# Overview of PMSM control strategies in electric vehicles: a review

Osman Emre Özçiflikçi<sup>1</sup> · Mikail Koç<sup>1</sup> · Serkan Bahçeci<sup>2</sup> · Selçuk Emiroğlu<sup>3</sup>

Received: 22 February 2023 / Revised: 12 September 2023 / Accepted: 13 September 2023 / Published online: 9 October 2023  
© The Author(s), under exclusive licence to Springer-Verlag GmbH Germany, part of Springer Nature 2023

## Abstract

Nowadays, permanent magnet synchronous machines (PMSMs) are preferred by electric vehicle manufacturers due to their attractive features, such as low acoustic noise, high torque/power density and higher efficiency and so on. In addition to these, qualities such as smooth torque production, wide range operation and less malfunctions are expected from electric vehicles. The realization of these features can be improved with the design of PMSM and their control strategies. In this study, PMSM control techniques that have been developed and are being developed in recent years in order to overcome the common challenges such as reduced torque ripples, efficiency optimization and simplified control algorithms are investigated. Therefore, the paper reviews the state-of-the-art drives in particular attention to smoother output torque, extended drive range, simplified control algorithms, less model dependency and so on. Also, recently developed techniques in stator and rotor topologies to reduce torque ripple are briefly reviewed.

**Keywords** Electric vehicle · PMSM · Torque ripple reduction · Control simplicity

## 1 Introduction

Electric vehicles (EVs) lead to prevent environmental pollution by reducing the use of fossil fuels and carbon dioxide emissions. [1–3]. Therefore, the use of EVs has become quite widespread and it is desired to be further spreaded. One of the important components to choose for EVs is the type of electrical machine to be employed in the vehicle. There are many studies in the literature for the selection of machines to be used in EVs [4–6]. In [4], the authors investigated the use of induction machines (IM), switched reluctance machines (SRM), brushless DC machines (BLDCM) and

permanent magnet synchronous machines (PMSM) in EVs. Each machine type has been studied in detail in terms of torque ripple, control techniques, etc. As a result, PMSM is highly preferred by various vehicle manufacturers and can be an alternative solution for EVs to be produced in the future. Similarly, the pros and cons of using IM, PMSM and SRMs in EV applications are presented in [5]. PMSM has been used in most electric vehicles manufactured between 2010 and 2020. As can be deduced from these studies, PMSM has been an attractive machine type for EV applications with their promising features.

PMSMs are superior to other machines due to their better operational performance, such as their wide speed range, high efficiency, high power density, [7–9]. Robust control techniques should be applied to them in order to properly utilize from their superior features. Conventionally, field oriented control (FOC) technique is used for the control of PMSMs [10–13]. In addition, the direct torque control (DTC) technique is also widely used for PMSM control [14–17]. FOC techniques are based on the principle of controlling -dq axis currents by using Park and Clark transformations. Unlike FOC, the control variables are torque and the amplitude of the stator flux vector in DTC drives. There are several studies in the literature that compare these techniques with each other and technical details are also given in [18, 19]. Recently,

✉ Osman Emre Özçiflikçi  
osman.ozciflikci@ahievran.edu.tr

Mikail Koç  
mkoc@ahievran.edu.tr

Serkan Bahçeci  
sbahceci@erciyes.edu.tr

Selçuk Emiroğlu  
selcukemiroglu@sakarya.edu.tr

<sup>1</sup> Electrical-Electronic Engineering, Kırşehir Ahi Evran University, Kırşehir, Turkey

<sup>2</sup> Electrical-Electronic Engineering, Erciyes University, Kayseri, Turkey

<sup>3</sup> Electrical-Electronic Engineering, Sakarya University, Sakarya, Turkey

model predictive control (MPC) [20–22] and deadbeat predictive control (DBPC) techniques [23–25], which can be built on both FOC and DTC, are also used in the literature. It is based on predicting the next state of the system in both MPC and DBPC techniques. The next state is predicted based on the machine models in discrete time. Some of the reasons why many different control techniques have been developed in the literature are the necessity of reducing the torque ripple for smooth torque production, increasing the battery utilization providing control simplicity and ensuring high efficiency operation. The control strategies developed in the literature in terms of solving aforementioned problems in real-life experiments have been reviewed from this perspective in this paper.

PMSMs can be divided into two groups, as surface-mounted PMSM (SPM) and interior-mounted PMSM (IPM) [26, 27]. The difference between SPM and IPM is the machine saliency ratio. Therefore, while IPMs are capable of producing reluctance torque, SPMs produce torque that can only be obtained from magnets. Due to the reluctance torque component, there is a difference in the determination of reference values of SPM and IPM drives [28]. Although FOC and DTC techniques are used for both types of PMSM, a different strategy should be applied in generating commands for efficient operation. Hence, while the  $-d$  axis current is kept at zero and the control is provided with the  $-q$  axis current for SPMs, the maximum torque per ampere (MTPA) strategy should be applied for IPMs in the constant torque region (CTR) [29–31]. In the constant power region (CPR), a field weakening (FW) strategy is developed for both machine types, and high-speed operation is performed by weakening the flux value [32, 33]. In both MTPA and FW strategies, it is necessary to generate commands based on the mathematical equations [34, 35] or pre-prepared look up tables (LUTs) [36]. Actually, a series of experiments is required in preparing LUTs or mathematically pre-calculated values must be defined in the processor. It can be deduced that using mathematical equations and LUT-based techniques are both a computation based on machine parameters. In addition, different methods designed to perform MTPA and FW operations regardless of parameters such as signal injection methods, search-based techniques, and feedback FW technique are discussed in this paper.

The command values to be produced based on the MTPA and FW equations (current values for FOC, the amplitude of the stator flux vector for the DTC technique) directly affect the performance of the system. The torque demanded by the drive may differ from the calculated value due to malfunctions in the processor or due to computational burden and memory problems. In this case, the performance of the vehicle may decrease. Hence, the determination of command values is an important challenge. Since the calculations in the MTPA and FW strategies directly use the machine parameters, it is crucial to know the parameters of the machine

accurately [37]. Also, model-based drive algorithms need to know the machine parameters, such as MPC or DBPC. Therefore, model-independent drives have been developed using the parameter estimation techniques in the literature [38–40]. Parameter estimation techniques are also discussed in the paper.

Even if existing control algorithms are improved by using the parameter estimation techniques or making the improvements on MTPA and FW calculations, simplicity of the control algorithms is also crucial for the drive. Hence, another criterion to be considered in the evaluation of algorithms developed in the literature is control simplicity. For example, the position sensor is removed from the system in order to achieve the control with less component [41–43]. However, although sensorless control algorithms provide the benefits to the system in terms of cost, it is expected that the control algorithm is not complex and has no disruptive effects on the drive. In fact, even if a newly improved control algorithm is simple, if the torque ripple increases, or if it decreases the battery utilization or makes it model dependent, all features of that algorithm should be considered with associated cons as well. Developed control algorithms are also compared with each other from this perspective.

Section 1 presents the studies performed to reduce torque ripple in PMSM design and control techniques. Also, the studies on battery utilization and torque ripple reduction with modulation techniques are examined. In Sect. 2, studies in the literature on MTPA and FW calculations related to the accuracy of system commands have been reviewed. Model-dependent and model-independent drives and parameter estimation techniques in the literature are reviewed in Sect. 3. In Sect. 4, the control simplicity of the techniques is discussed.

## 2 Torque ripple reduction and battery utilization ratio

Torque ripple reduction can be achieved by two ways: machine design and improvement of control algorithms. Also, the increase in the battery utilization ratio is related to the control. In this section, the state-of-the-art studies on reducing torque ripple with machine design, current studies on reducing torque ripple with the improvement of control algorithms, and control algorithms developed for the increase in battery utilization ratio are investigated.

### 2.1 Design approaches for reduced torque ripple

Reducing the torque ripple and increasing the efficiency of the PMSM first starts with the design of the machine. With the change of magnetic materials used in the production of PMSMs, improvements in the stator, and different designs in

the rotor topology, it is possible to reduce the torque ripple and increase the efficiency by reducing the losses [44–51]. If the studies on rotor topology and magnet types are examined, article [44], it is aimed to increase the torque density and decrease the torque ripple by optimizing magnet pole shape in the rotor. The magnet pole embrace, magnet height, and pole arc angle are optimized with the help of an optimization algorithm. The new machine obtained produced lower torque ripple under rated torque and speed conditions than the baseline machine studied. In [45], a combination of V-type magnet rotor and spoke-type rotor is proposed to obtain maximum efficiency and low torque ripple without sacrificing torque density. A new Y-type rotor was designed by taking advantage of the high torque density of the V-type rotor and the low torque ripple of the spoke-type rotor. As a result, the similarities of Y-type IPM with the Toyota Prius machine were revealed and a hybrid machine with low torque ripple and high torque density was designed. In [46], a novel machine is proposed using a lower cost magnet, which can have the same torque ripple and average torque as the conventional SPM. While the torque ripple and average torques of the proposed machine and the conventional SPM are approximately similar, the production cost of the machine has been reduced. In [47], a high performance machine design has been proposed by using hybrid magnet types. As a result, the torque ripple of the proposed machine at the maximum torque operating point is lower than that of the target machine. From this it can be deduced that changing the magnet type has an effect on the torque ripple. Considering the improved machine designs related to the stator, in [48], an IPM with low torque ripple is designed for electric vehicles. Since the torque ripple is highly dependent on the stator windings, the winding type is chosen as distributed type to reduce it as much as possible. In [49], the authors carried out work on stator slots for the prevention of torque ripple and rotor eddy losses. When comparing open and closed stator slot machines. It was observed that the closed slot structure reduces the torque ripple extremely. Also, there are studies in the literature that have been made to find the optimum number of slots and poles and that the torque ripple can be reduced to lower levels [50, 51].

### 2.2 Control strategies for reduced torque ripple

Independent of the control algorithms, the drive design is performed based on the machine modeling in (1–8). Current control loop of various FOC-based control strategies is given in Fig. 1, torque and stator flux amplitude loop of DTC-based control strategies are given in Fig. 2. The current values obtained by applying MTPA and FW strategies are taken as a reference in order to perform the torque control in the drives given in Fig. 1. In fact, it is sufficient to provide the current control loop to observe the difference between these

techniques. The difference in speed-controlled drives is that command currents are produced only from the error in the speed information. In other words, there is an external control loop in speed-controlled drives. For both the FOC-based techniques given in Fig. 1 and the DTC-based techniques given in Fig. 2, the speed-controlled drive design has been carried out using Eq. (8) with the help of a controller.

$$V_d = R * i_d + \frac{d\Psi_d}{dt} - \omega * \Psi_q \tag{1}$$

$$V_q = R * i_q + \frac{d\Psi_q}{dt} + \omega * \Psi_d \tag{2}$$

$$\Psi_d = \int [V_d - R * i_d + \omega * \Psi_q] \tag{3}$$

$$\Psi_q = \int [V_q - R * i_q - \omega * \Psi_d] \tag{4}$$

$$i_d = \frac{\Psi_d - \Psi_m}{L_d} \tag{5}$$

$$i_q = \frac{\Psi_q}{L_q} \tag{6}$$

$$T_e = \frac{3 * p}{2} [\Psi_m * i_q + (L_d - L_q) * i_d * i_q] \tag{7}$$

$$\omega_m = \int \frac{T_e - T_m - B * \omega_m}{J} * dt \tag{8}$$

There have been several studies in the literature recently to reduce torque ripple in PMSMs driven by FOC technique as can be seen in Fig. 1a [52–55]. In [52], a novel drive is proposed to reduce the torque ripple of a PMSM used in compressor applications and to reduce DC link voltage fluctuations. The drive improved to reduce torque ripple has been validated by experimental results. It has been observed that the speed-controlled compressor drive reduces speed fluctuations. In article [53], it is aimed to reduce torque disturbance by working on an extended harmonic state observer. The design of the extended harmonic observer is complex because it includes a closed-loop control system. With the robustness of the developed harmonic observer and suppression of ripples, the proposed harmonic observer has been verified. It has been stated that the complexity of the harmonic observer increases with the increase in the number of harmonics, and it is mentioned that there may be studies to be focused on in the future. In [54], a drive in which the -q axis current is produced by using iterative learning controller and adaptive sliding mode controller together has been proposed, instead of the controller in which the iterative learning control and PI regulator are used in parallel, which are conventionally used in the speed controller. It has been verified by experimental results that the proposed speed controller minimizes torque ripple compared to other controllers. As a result, torque ripple

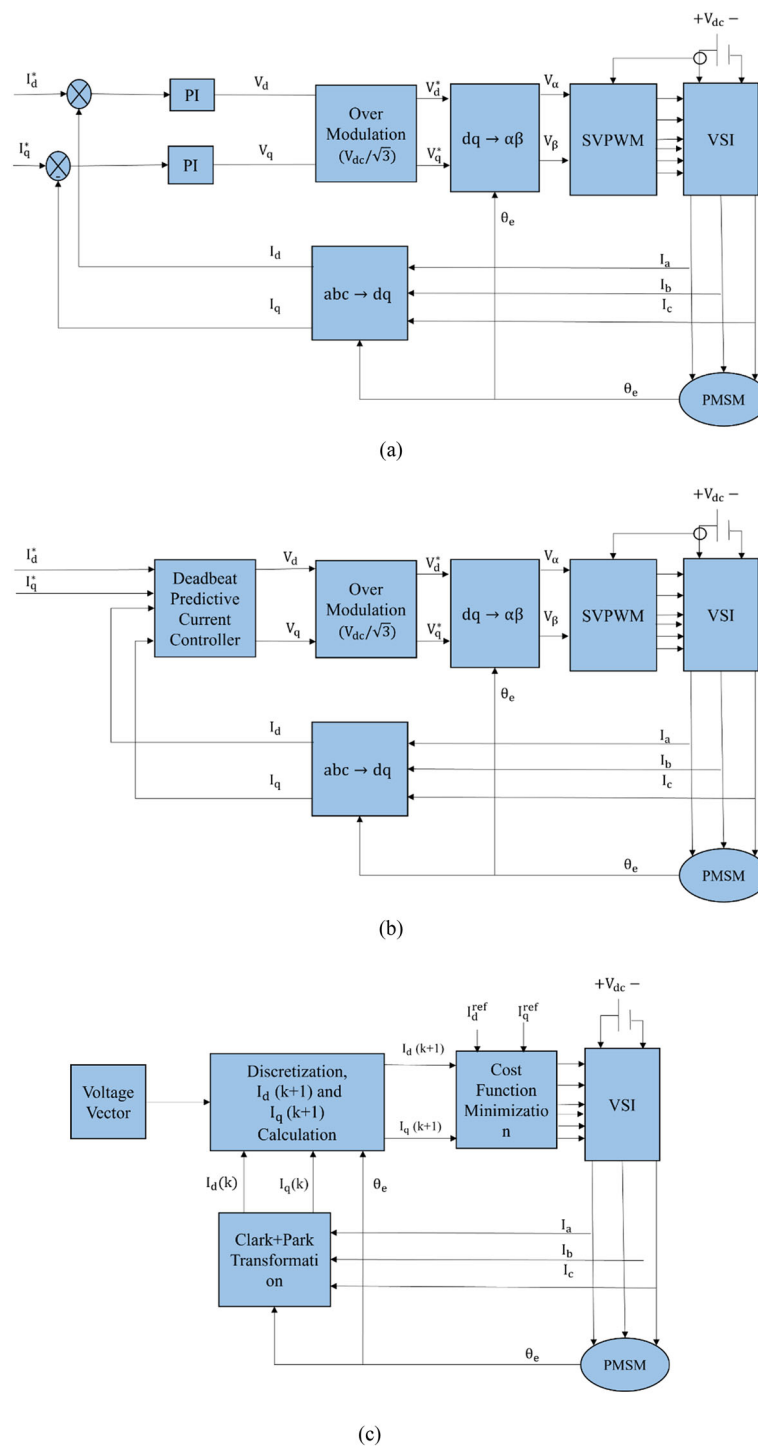


**Fig. 1** **a** Simple FOC technique. **b** FOC Based DPCC technique. **c** FOC Based MPC technique

is minimized by developing the speed controller. Similarly, in [55], the authors minimized torque ripple by developing current loop controllers in a speed-controlled PMSM drive. In addition, it has been experimentally proven that the torque ripple is reduced by comparing the conventionally used PI controllers in the current loop with the linear active

disturbance rejection controller (LADRC) and the proposed enhanced LADRC.

DTC is developed as an alternative to FOC technique as can be seen from the schematic of DTC-based different control techniques in Fig. 2. DTC technique can be divided into two groups as hysteresis-based DTC (HB-DTC) [17, 56–58]

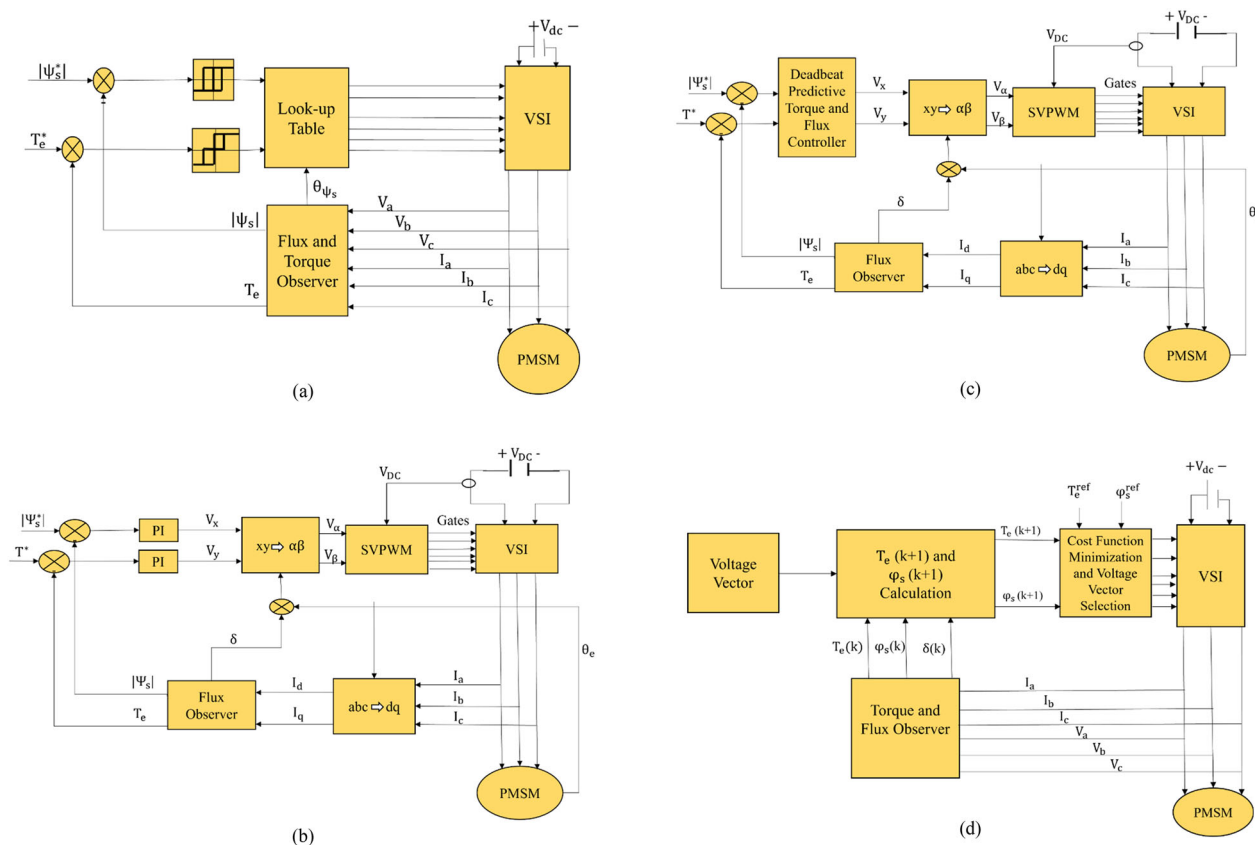


Fig. 2 a HB-DTC Technique, b SVM-DTC. c Deadbeat predictive torque and flux controller based DTC. d MPC-based DTC technique

using hysteresis controllers and pulse width modulation-based DTC (PWM-DTC) [15, 59]. The HB-DTC technique is used as an alternative to FOC, since it does not use a position sensor and reduces the drive cost. But contrary to the advantage of no position sensor, too much torque ripple is observed in the drive [59]. In addition, the fact that the switching frequency is not constant, the torque ripple increases. PWM-DTC technique has been developed to overcome the mentioned problems. However, because of the necessity of using Park and Clark transformations in PWM-DTC technique, there must be a position sensor [15]. Hence, when choosing the control strategy, all the features of the drive such as cost, torque ripple should be taken into account.

Like torque ripple reduction studies in FOC control, the HB-DTC technique has also been studied on torque ripple reduction [16, 17, 56, 60]. In [16], it is aimed to achieve sensorless speed control with a sliding mode controller. In addition, the conventionally used 3-level hysteresis controller for the torque component is designed as 7-level. It is confirmed by simulation results that the proposed drive reduces torque ripple. In article [56], it has been proven that current harmonics are suppressed by modifying the switching table with the proposed method. Hence, suppression of current

harmonics can be effective in directly torque ripple reduction. A novel duty-based HB-DTC technique is proposed in [60]. It has been confirmed by experimental results that the proposed drive provides less torque and flux ripple compared to the conventionally used HB-DTC technique. It has also been reported that the average switching frequency is lower. Unlike other studies, matrix converter fed drives using multidimensional switching table for common mode voltage minimization has been proposed in [17]. Although the common mode voltage is minimized with the proposed method, it is stated that the torque ripple is higher than the conventional DTC. Therefore, it should be studied by taking into account the negative effects of a part developed in the control system on the drive. In addition, since the HB-DTC technique produces high torque ripple, PWM-based DTC techniques developed to deal with this are also widely researched [59, 61, 62].

Model predictive control (MPC) and deadbeat predictive control (DBPC) techniques are also widely used in the literature. MPC and DBPC techniques can be applied to both FOC and DTC techniques as can be seen from Figs. 1 and 2 [22, 25, 61, 63–65]. The MPC technique basically has a cost function that finds the optimal voltage vectors for the inverter. By minimizing the cost function, the error is reduced and the



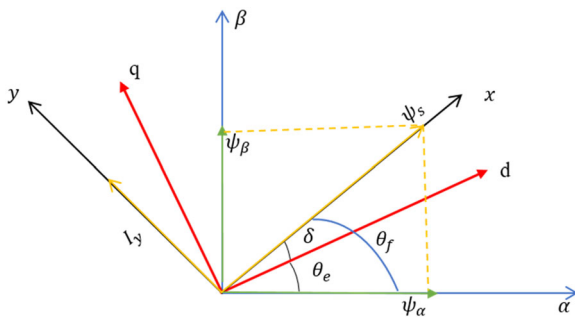


**Fig. 3** Stator and rotor oriented coordinate system

switching signals are selected accordingly. In DBPC, derivative expressions in machine equations are defined in discrete time, and control is provided by using predictive technique. The main purpose of these techniques is to remove the PI controllers from the drive whose parameters need to be adjusted in the system. However, the system's computational burden [64] and torque ripple increase [66, 67] in drives using MPC or DBPC techniques. In [61], the novel deadbeat DTC drive is proposed, reducing the computational burden and torque ripple. When comparing conventional PI-based DTC technique, conventional deadbeat DTC technique and proposed drive in the study, it is an important result that torque ripple and current distortions are more in PI-based DTC. Also, the torque ripple of the novel deadbeat DTC drive proposed in the study is lower than that of the drive using FOC, PI-based DTC, and conventional deadbeat DTC. In [63], a drive is designed to suppress the current harmonics of the FOC-based deadbeat controller. By performing tests of the designed drive at different speeds, it has been shown that the current harmonics decrease when the proposed drive is applied. Although the torque ripple comparison is not made in the scenario where the proposed technique is applied and not applied, the low total harmonic distortion in the currents directly reduces the torque ripple. A drive with a low computational burden has been proposed by using the stator-oriented coordinate system ( $-xy$  frame) instead of the rotor-oriented coordinate system ( $-dq$  frame) for the calculation of the deadbeat controller built on the DTC in [64]. The  $-dq$  and  $-xy$  frame difference can be seen in Fig. 3. The lower torque ripple and lower computational burden in the proposed drive have been confirmed by experimental results.

In [22], it is aimed to reduce torque ripple, current distortions and switching frequency by performing a novel particle swarm optimization (PSO) algorithm-based optimization on the weighting factors of the cost function minimized in MPC. It has been verified by experimental results that the drive operated with the adjusted factors with the proposed PSO algorithm produces less torque ripple. Similarly, in [65], the weighting factors are optimized with genetic algorithm and artificial neural networks in the MPC drive. Experimental and

simulation studies have confirmed that current distortions, hence torque ripple, decrease. Also, the modulated model predictive control technique (MMPC) has been presented in the literature. Due to the fact that the switching frequency is not constant in the MPC technique and the torque ripple is high. In [68] MPC and MMPC are compared with each other. Total harmonic distortions (THD) in the stator currents are calculated in both techniques in response to different torque commands. The current distortion of the drive using the MMPC technique has turned out to be dramatically low. Accordingly, the torque ripple of a drive constructed with the MMPC technique is considerably lower than the one constructed with the MPC technique. Techniques developed to provide control simplicity, and torque ripple of the MMPC technique are available in the literature [69, 70].

### 2.3 Torque ripple reduction with improved PWM strategies and battery utilization rate

Following the review of control strategies and the discussion of reducing torque ripple with different control techniques, the drive's switching strategy also needs to be specifically addressed in order to achieve lower torque ripple. The high frequency operation of the power switches in the inverter structure reduces the torque ripple and increases the inverter losses. Determining the optimum operating conditions for the inverter by considering the trade-off between the two cases is also an important subject of study. PWM signal generator is required for inverter regardless of whether it is FOC- or DTC-based drive. As mentioned in the control strategies section, considering that PWM-DTC is better than HB-DTC and MMPC is better than MPC in terms of torque and current ripples, it reveals the importance of the PWM strategy.

The sinusoidal PWM (SPWM) technique, which is the most basic PWM technique, is widely used in the literature [71, 72]. However, it is not a superior strategy due to low battery utilization ratio, high switching losses and high current distortions for machine drive systems. The third harmonic injection PWM (THIPWM) strategy is an alternative technique to increase the battery utilization level [73]. Even though the THIPWM strategy is a PWM strategy based on the SPWM strategy, its battery utilization ratio is about 15.5% higher than SPWM. Due to the high switching losses of the THIPWM strategy and the high THD ratio, the space vector PWM (SVPWM) strategy has been developed. Space vector PWM (SVPWM) strategy is frequently used in recent machine drives due to its superior features, such as high battery utilization ratio, low switching losses, and low THD ratios [7, 74]. Also, studies have been carried out to increase the battery utilization ratio, to decrease the computational burden [75], and to reduce the switching losses of SVPWM in the literature [76]. In [75], an SVPWM method has been

proposed to change the medium vector with a fixed 30° sector angle by increasing the number of SVPWM sectors to 12. The proposed SVPWM technique for two inverters has been tested in a dual three-phase PMSM system. As a result of the real-time experiments, it has been revealed that the computational burden is less, and it produces less current harmonics compared to the 6-phase conventional SVPWM. Similar to the work in [75], duty cycle optimization was carried out in order to develop the SVPWM strategy in the dual PMSM drive in [76]. It is more complex as there are only eight voltage vectors for SVPWM in 3-phase PMSMs, while dual PMSMs have 64 voltage vectors. However, the average switching frequency has been reduced with the duty cycle optimization technique, which has been verified by real-time experiments. Normally, in the SVPWM strategy, zero vectors are active during the waiting times in each PWM period, while in the proposed technique, the waiting times of the zero vectors are optimized, and the switching frequency is reduced. Therefore, torque ripple and inverter losses are also reduced.

There are also studies in the literature to increase the drive range by improved battery utilization ratio. The battery utilization ratio can be increased by developing PWM techniques [77] or developing overmodulation strategies for any FOC [78–80] and DTC [81] driven PMSMs. The conventionally used carrier-based PWM technique have been improved with the idea of a virtual duty axis. A PWM strategy with a lower switching frequency and a lower computational burden have been developed in [77]. Also, the overmodulation strategy has been adapted to be more robust in the operations in the overmodulation region for the PWM strategy. Thanks to the overmodulation strategy, it was observed that the DC bus utilization ratio increased compared to the carrier-based PWM technique used conventionally. Overmodulation strategies are applied to take full advantage of the voltage hexagon as can be seen in Fig. 4. In this way, it is desired to maximize battery utilization. However, dynamic overmodulation strategies have been presented in the literature according to operating conditions as long as the machine is in operation.

In [78], it is proposed to compensate for the variations depending on the rotor position in the overmodulation strategy so that the control performance can be well maintained rather than maximizing the voltage usage. Experimental results have confirmed that control performance is permanently maintained in the over-modulation region regardless of rotor position. [79] discusses an overmodulation strategy on suppressing voltage jumps and current harmonics when operating in the overmodulation region at high speeds. The regions outside the voltage hexagon are divided into sub-regions and different durations are generated for each region. Then, the sector and  $T_0, T_1, T_2$  are determined and switching signals are generated. The proposed strategy has increased

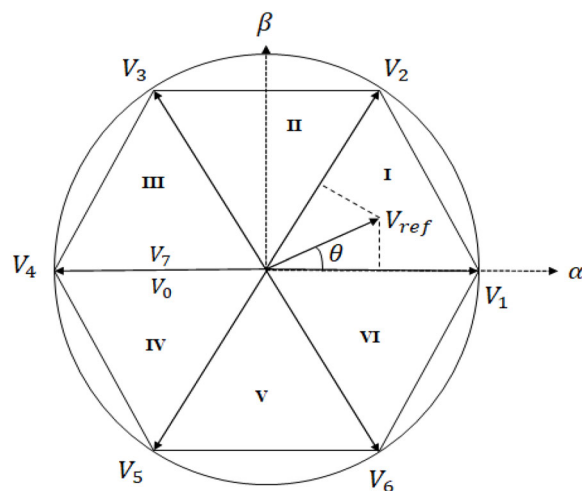


Fig. 4 Voltage hexagon

DC bus utilization ratio and modulation index. This strategy has been validated by real-time experiments on SPM machines where voltage drop and current harmonics are suppressed. DC bus utilization ratio has been increased in [80] by using the double voltage vector technique instead of the virtual voltage vector technique, which is conventionally used to drive 5-phase PMSMs in MPC-based drives where the control variables are currents (FOC). It is presented that while the DC bus utilization ratio is limited in the virtual voltage vector technique, it is fully used in the proposed technique. In [81], it was aimed to reduce torque ripple and increase DC bus utilization ratio by optimizing the switching table in the HB-DTC technique. As a result of simulation and real-time experiments, it was observed that torque ripple decreased and DC bus utilization was improved. Also, it has been mentioned that this drive is suitable for electric vehicles with low torque ripple and high DC bus utilization.

### 3 Accuracy of command

This section will focus on the techniques required to achieve the speed or torque demanded from the drives with maximum efficiency in PMSM constant torque and constant power region operations. Firstly, the MTPA strategy used to increase efficiency in IPM machines is detailed. Then, the FW technique, which is used for both machine types at high speeds, is discussed. These techniques play an important role in determining drive commands, and well-designed MTPA and FW strategies greatly affect drive efficiency. Figure 5 shows how the MTPA and FW strategies are implemented in both FOC-based and DTC-based drives. Torque input is applied to the MTPA and FW block in Fig. 5. If the drive is speed controlled, the torque value obtained from the outer control loop

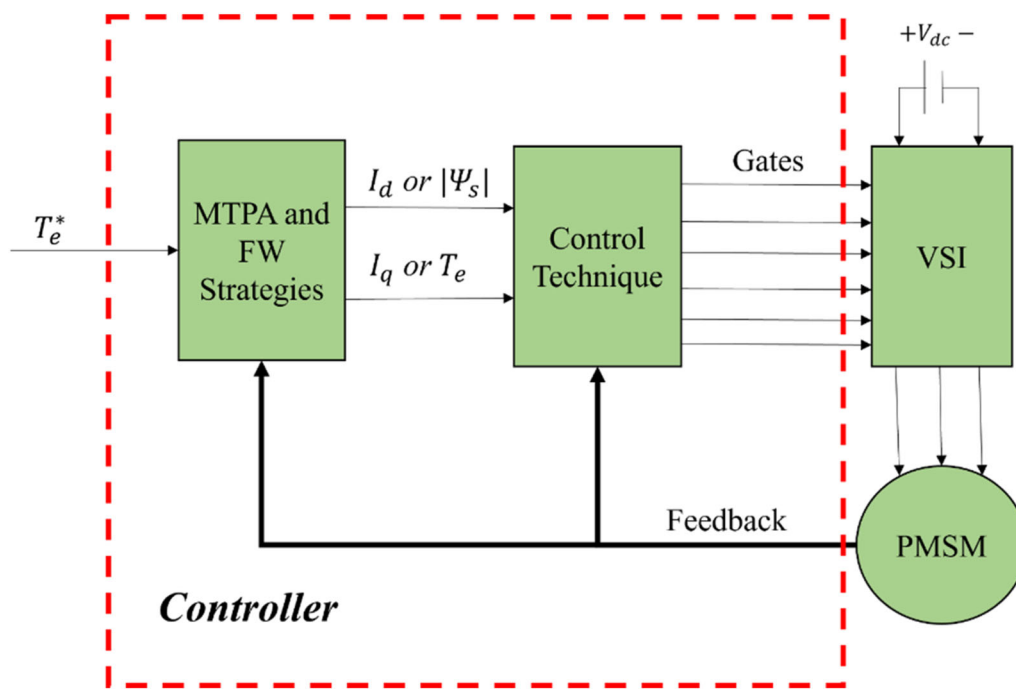


Fig. 5 Implementation of MTPA and FW strategies

is used. Using the  $-dq$  axis currents obtained after the calculations, the stator flux amplitude required for the DTC is obtained by machine equations.

### 3.1 MTPA strategies

It has been shown in detail in [28] that the conventionally used  $I_d = 0$  control technique is inefficient due to the different  $-dq$  axis inductances in IPM machines. Higher torque capacity can be achieved by accurate control of the reluctance torque component, which depends on the inductance in the torque equation. Also, according to [28], the commands according to  $I_d = 0$  puts the machine in the FW region earlier and reduces the use of torque capacity. Therefore, the implementation of the MTPA strategy on IPM machines is vital for drive efficiency. The purpose of applying the MTPA strategy is to minimize the copper losses by calculating the optimum  $I_d$  and  $I_q$  currents corresponding to the torque demanded from the system. Therefore, the  $\beta$  angle equation given in (10) must be solved in such a way as to provide the minimum current. After obtaining the  $\beta$  angle,  $I_d$  and  $I_q$  currents are obtained by using Eqs. (9, 11, 12). However, although the equation is correct in theory, since the motor parameters also depend on  $I_d$  and  $I_q$  currents, this equation may deviate from the optimum angle depending on parameter variations in real-time applications.

$$I_d = -I_s * \sin \beta \quad I_q = I_s * \cos \beta \quad |I_s| = \sqrt{I_d^2 + I_q^2} \quad (9)$$

$$\beta = \sin^{-1} \left( \frac{-\Psi_m + \sqrt{\Psi_m^2 + 8(L_q - L_d)^2 I_s^2}}{4(L_q - L_d) I_s} \right) \quad (10)$$

$$I_d = \frac{\Psi_m}{2(L_q - L_d)} - \sqrt{\frac{\Psi_m^2}{4(L_q - L_d)^2} + I_q^2} \quad (11)$$

$$I_q = \left( \frac{3p}{2} \right)^{-1} \frac{T_e}{\Psi_m - I_d(L_q - L_d)} \quad (12)$$

In the implementation of MTPA strategies, it can be divided into four categories as mathematical equations [74, 82], look-up table (LUT)-[36, 83] based methods, signal injection [84–86] and search algorithms [87, 88]. The main reason for categorizing MTPA strategies in this way and developing these techniques is to provide simplicity of control, and to find the accurate MTPA trajectory by eliminating model dependence.

An efficient FOC-based drive was created by solving MTPA mathematical equations with Newton Raphson iteration method in [74]. The main purpose of the study is to compare the computational burden of two drives with a look-up table (LUT)-based MTPA and an MTPA strategy with Newton Raphson iteration method. As a result of simulation studies, it has been confirmed that the computational burden of look-up table LUT-based MTPA is lower. It has been investigated that more than one SPM machine can be controlled with a single inverter in [82]. Also, each machine is operated in isolation from each other and there is no power



flow between them. One machine is closed loop controlled, other machines are open loop controlled and detailed calculations are made to ensure synchronization between them. In finding the MTPA point, the  $I_d$  current has been obtained by using the Lagrange Multiplier method by writing the equations through the Joule losses. The subject of parameter variations poses a problem and is stated in the conclusion as future studies.

In [36], current measurement sensors have been removed from the drive, aiming for a low-cost and simpler drive design. MTPA calculations are performed with voltages and applied with a LUT in order to reduce the computational burden. It has been stated that the proposed method can also be implemented with the online solution of the given quadratic equation. As a result of real-time experiments, the effectiveness of the system designed without using current sensors has been verified. In [83], drives with  $I_d = 0$  control, LUT-based MTPA and virtual signal injection-based MTPA strategy have been compared for electric vehicles with particular attention to noise and vibration. From the experimental results, it is deduced that the efficiency can be increased and noise can also be improved in EVs where virtual signal injection-based MTPA strategy is applied.

The online solution of mathematical equations for MTPA or the application of LUT-based MTPA strategies are not robust techniques due to nonlinear machine parameters. MTPA strategies protected against changing parameters have been achieved by the use of signal injection and search algorithms. Signal injection techniques can be divided into two groups as real signal injection and virtual signal injection. Since the real signal injection techniques increase the drive losses and reduce the efficiency as the signal is applied externally. So, virtual signal injection has been developed, where the signal injection is performed by making mathematical calculations. However, the real signal injection method proposed in [84] finds MTPA points better than the virtual signal injection method. In addition, virtual signal injection methods increase the computational burden. Hence, the choice should be made according to what compromises will be made in the methods to be used.

If [83] is reconsidered, the drive with virtual signal injection is more efficient and noiseless than  $I_d = 0$  controlled and LUT-based MTPA-based drive, and real signal injection also increases losses and causes low efficiency. Certainly, studies continue for the improvement of virtual signal injection in the literature. For example, in [85], the performance of the drive is increased by estimating inductance values using a parameter estimation technique of the machine parameters it uses based on virtual signal injection. The virtual signal injection technique developed in [86] estimates the derivative expressions of the machine parameters. With the proposed technique, it can automatically compensate for the error caused by these derivative terms before enabling the

virtual signal injection. Thus, the drive successfully achieves the MTPA operation even if the machine parameters are unknown.

Another technique used to find the MTPA trajectory is search algorithms. Since there is parameter dependence in the calculation of the reference value of the stator flux amplitude in the hysteresis-based direct torque control drive system, it is aimed to find the MTPA points with the extreme seeking control (ESC) technique in [87]. A new ESC with signal injection and the use of filters has been proposed. Since PI is used while applying ESC, the values of the control parameters are important. For this reason, the setting of parameters in the closed-loop control used in the reference selection of the ESC is also emphasized. The results of the flux observer and the ESC have been plotted and compared, and it has been observed that the drive was working correctly. It is confirmed by the results to be a robust HB-DTC drive against parameter changes. In [88], perturbation and observation techniques have been applied to find MTPA points without parameter errors in the control of dual machines with a mono inverter. MTPA is successfully found by arranging the  $\theta_d$  angle generated from machine equations using perturbation and observation algorithms. In the instantaneous change of machine speed and load torque, the algorithm is provided to perform continuous perturbation with a perturbation step, whose convergence rate is determined to be very low. A parameter-independent MTPA scheme has been validated by simulation studies and real-time experiments.

### 3.2 FW strategies

PMSMs generally have two different operating regions: constant torque region (CTR) and constant power region (CPR). The machine is driven in the most efficient way by using different strategies for two different operation regions. CTR is the operating region below the base speed of the machine and in this region the machine is controlled using the MTPA strategies mentioned in the previous section. If the machine is operating above the base speed value, the machine is driven by applying a field weakening (FW) strategy by reducing the amplitude of the  $-d$  axis current [89] or flux component. The machine used in electric vehicle is expected to provide the desired torque from the vehicle in a wide speed range. Ensuring the control of the machine only in the CTR is not sufficient for electric vehicle applications, as it causes the entire capacity of the machine not to be used. In order to the torque and speed capacity of the machine to be used efficiently, MTPA and FW strategies must be applied in the drive for wide operating region.

When the machine is operated above the base speed, the MTPA strategy cannot meet the current and voltage limits [90]. Therefore, the FW strategy should be used in CPR to meet current and voltage limits. The FW strategy, which is

implemented with a feedback control loop using the measurements of the reference voltages from the inverter output, is called feedback FW, and the method that calculates the FW flux or -dq axis currents through the equations based on the machine model is called feed-forward FW [33]. In the feedback FW strategy, it is not dependent on the machine parameters, as the calculation is performed with the reference voltages at the inverter output. However, since a control system is created, it has problems such as adjusting its parameters and determining the bandwidth. Unlike the feedback FW strategy, the feed-forward FW strategy is directly dependent on machine parameters as it is model based. Therefore, the inability to specify the parameters correctly will result in poor performance in FW operations. In [91], a feed-forward torque controller is proposed by mentioning that the torque of the machine and the reference torque may differ from each other due to the error in the angle in the sensorless PMSM drive. Particularly since this difference will cause instabilities in the FW region, the FW region has been improved in the study. The robustness of the proposed method has been verified by simulation and experimental study results by applying both the feedback FW strategy and the LUT-based FW strategy. A deadbeat current controlled drive is designed for 5-phase PMSM using a modified SVPWM scheme in [92]. In the solution of the machine equations in the feed-forward FW strategy, the -d axis current has been obtained by using the gradient descent optimization technique. Since the voltage limit is set manually in the conventionally used FW strategies, it causes the wrong limit in the FW region and this causes harmonic formation. This problem was solved by optimizing the -d axis current online with the gradient descent method. In [93], the operation is carried out in the FW region by applying the feedback FW strategy. In order to develop the feedback FW strategy, without the need for DC voltage measurement, the modulation index is obtained with the help of filtering over  $S_a$ ,  $S_b$ ,  $S_c$  switching signals and the maximum modulation index is determined as 1, and the error between them is fed to the PI regulator and the  $I_d$  reference is created. It has been confirmed by experimental studies that the transition performance in the FW region is smooth. However, a missing aspect of the study is the modulation index is calculated by ignoring the nonlinearity of the inverter.

## 4 Model dependency and control simplicity of drive

### 4.1 Model dependency

It can be seen from (1–8) that -dq axis inductances, flux linkage and stator resistance values are used in machine equations. Hence, it can be seen that directly depends on

the parameters FOC technique, DTC technique, and since it discretizes the machine equations for MPC and deadbeat technique from (13–23). In addition to these, the calculation of commands to be requested from the drive, namely MTPA and FW strategies, is also based on parameters. As mentioned, the parts developed both in the MTPA and FW strategies and inside the controller are depicted in Fig. 6. Therefore,  $L_d$ ,  $L_q$ ,  $\Psi_m$  and  $R_s$  values must be correctly defined in the drive. However, the machine parameters change instantaneously with magnetic saturation, temperature and similar effects. Either these parameters need to be measured, stored, and used by real-time experiments, or these parameters need to be tracked with parameter estimation techniques. In this study, a brief review is made on the numerical online parameter estimation techniques, which have been widely used in recent years.

Recursive least square (RLS) [37, 38, 94], model reference adaptive system (MRAS) [85, 95], Luenberger Observer (LO) [96], and extended Kalman filter (EKF) [97, 98] are widely used techniques for online parameter estimation. In [37],  $L_d$ ,  $L_q$  and  $\Psi_m$  parameters have been estimated with the recursive least square estimation technique in order to make the MTPA strategy and decoupling compensation in the FOC parameter independent, and the gap between the reference torque and the actual torque has been closed in the results. By using the sinusoidal signal injection method, it is possible to cope with the rank deficiency problem. Similarly, MTPA strategy has been developed by estimating  $L_d$ ,  $L_q$ ,  $\Psi_m$  and  $R_s$  parameters with RLS technique in order to improve torque control in [94]. Also, similar to [37], a sinusoidal current injection strategy was applied to solve the rank deficiency problem. In [38], a controller with better performance has been obtained by estimating  $L_d$ ,  $L_q$ ,  $\Psi_m$  and  $R_s$  parameters with RLS in order to obtain a parameter independent drive of a PMSM speed controlled with MPC technique.

$$V_d = V_d^* - \omega_e * \Psi_q \quad (13)$$

$$V_q = V_q^* + \omega_e * \Psi_d \quad (14)$$

$$\Psi_d = L_d * I_d + \Psi_m \quad (15)$$

$$\Psi_q = L_q * I_q \quad (16)$$

$$|\Psi_s| = \sqrt{\Psi_d^2 + \Psi_q^2} \quad (17)$$

$$\delta = \tan^{-1} \frac{\Psi_q}{\Psi_d} \quad (18)$$

$$T_e^* = \frac{3 * p}{2} * (\Psi_d * I_q - \Psi_q * I_d) \quad (19)$$

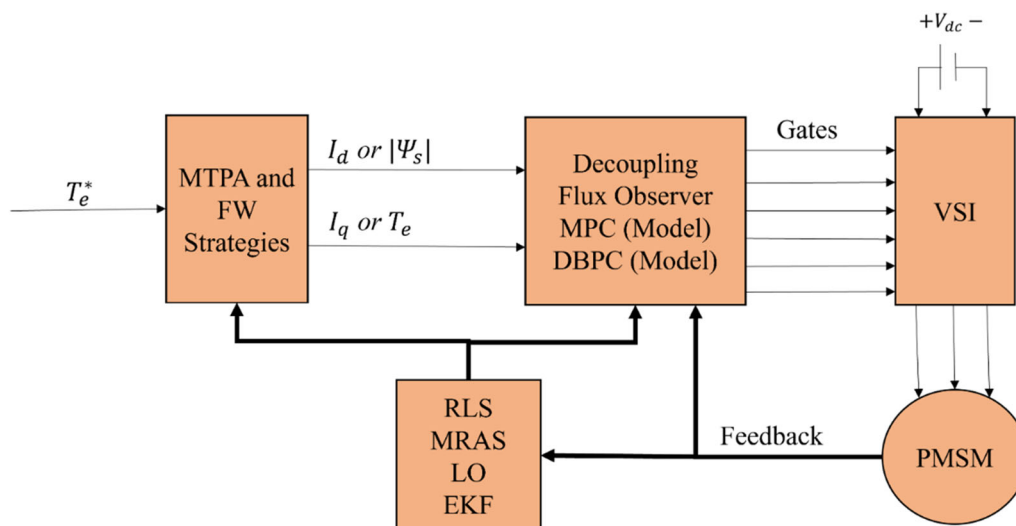


Fig. 6 Improvement of drive with parameter estimation techniques

$$\Psi_\alpha = \int (V_\alpha - R_s * I_\alpha) dt \tag{20}$$

$$\Psi_\beta = \int (V_\beta - R_s * I_\beta) dt \tag{21}$$

$$|\Psi_s| = \sqrt{\Psi_\alpha^2 + \Psi_\beta^2} \tag{22}$$

$$\theta_{\Psi_s} = \tan^{-1} \frac{\Psi_\beta}{\Psi_\alpha} \tag{23}$$

In the MTPA strategy performed using virtual signal injection in [85], it has been stated that the virtual signal injection strategy was dependent on  $L_d$ , and it has been aimed to estimate with the MRAS technique. It has been verified by simulation studies that the developed drive performs better in finding the MTPA trajectory. In [95], the  $R_s$ ,  $L$  and  $\Psi_m$  parameters obtained using the MRAS technique are fed into a new strategy in which MRAS and particle swarm optimization techniques, in which the inertia and damping coefficient can also be calculated, are used as a hybrid. From the simulation results, it has been shown that better parameter estimation can be made with the new MRAS-based technique. However, the drive has not been improved by using the estimated parameters in any part of the drive. In order to improve the deadbeat current control technique on the SPM machine, the  $R_s$ ,  $L$  and  $\Psi_m$  parameters have been estimated in [96] with the Luenberger observer. In the simulation and experimental results, when the parameters are different, there is a gap between the reference current and the actual current, while successful current control has been achieved with the applied technique, and the system is made parameter-independent. In [97],  $\Psi_m$  and  $R_s$  estimation has been performed with an improved EKF, since the process

noise in classical EKF is made according to Gauss and is not suitable for nonlinear systems. It has been verified from the simulation results that the estimation algorithm gives better results. In [98],  $L_d$ ,  $L_q$  estimation has been performed with EKF technique in a dual PMSM system with a single open phase fault. As a result of experimental studies, it has been verified that it is a robust prediction algorithm against the variation of machine torque and speed. In addition, the strategy is robust since the inverter nonlinearity is also taken into account in the implementation of EKF. In [99], the  $\Psi_m$  parameter of a sensorless controlled IPMSM with MRAS was estimated by EKF. The controller is made more robust by estimating the permanent magnet flux value used in sensorless control with MRAS. In addition, EKF and MRAS are commonly used techniques for sensorless control of PMSM [100, 101].

### 4.2 Control simplicity of drive

All the control techniques, command generation strategies, and parameter estimation techniques mentioned throughout the paper have been developed to increase control quality and improve drive performance. In the back-ground of all these improvements, it is absolutely necessary to consider that the total computational burden of the drive is not heavy, the cost is not high, and the strategies are easy to implement. If control techniques, the accuracy of commands, and parameter estimation techniques are emphasized, control simplicity can be summarized with the following items.

- Although the HB-DTC technique provides position sensorless control, it makes the drive inefficient of the components with variable frequency and high torque ripple.

- The PWM-based DTC technique has a fixed switching frequency and although the torque ripple is relatively lower, it has both HB-DTC and PWM-based DTC flux observer structure. Flux observer is vital in the drive and is parameter dependent. Therefore, it is necessary to use parameter estimation technique in the drive and the control algorithm is complex.
- In FOC- and PWM-based DTC, predictive control techniques have been developed because it is difficult to adjust the parameters of the controllers that will minimize the errors of  $-dq$  axis currents and torque-flux components in closed loop control. However, in both MPC and dead-beat control techniques, the drive is directly dependent on the model, as the next state estimation is made through machine equations. Eliminating parameter dependency and improving drive performance makes control more complex.
- Iteration-based techniques in MTPA strategies increase the burden of the microprocessor. In LUT-based techniques, memory problems may also be encountered in the microprocessor. Signal injection techniques increase the computational burden considerably, but they eliminate model dependency. If iteration-based techniques and LUT-based techniques are to be applied, a model-independent drive should be created using parameter estimation techniques. This will complicate the drive. In the selection of the MTPA strategy, preference should be made according to the drives requirements and application area.
- Similar to MTPA, if feed-forward FW is used, the parameter estimation technique should be used to increase control performance since there is model dependency. When using feedback FW, the PI regulator should be adjusted well.
- Since the parameter estimation techniques given in this paper are numerical online calculation techniques, they will impose a computational burden on the microprocessor when used. But the use of these techniques is necessary in order to know the parameters correctly, which is perhaps the most important topic for the drive. To make a comparison between the techniques, while RLS EKF and LO is more complex due to matrix calculations, MRAS seems relatively simple as it consists of comparing the adjustable model and the reference model and driving the error to zero with the PI regulator. Which technique to use should be chosen according to the application area and requirements.

## 5 Conclusion

In this study, state-of-the-art studies about PMSM in recent years have been reviewed. Unlike the review studies in the literature, a specific topics is not studied, and it is expressed

what the developed techniques and specific topics correspond to in real life especially on the electric vehicles. The main subject of this review is to extend the machine life, extend the drive range of the vehicle, reduce the computational burden of the microprocessor to work for a long time, and accordingly simplify the control strategy. Since the long machine life is highly dependent on the low vibrations. Hence, different control techniques have been developed to reduce the torque ripple, or the developed control techniques have been designed in different forms to increase the performance because the torque ripple is high. Similarly, control strategies are being developed to extend the battery usage in the vehicle in order to increase the range especially on switching strategies. Also, the techniques developed can complicate the drive even if they solve a problem. With this point of view, the burden of the microprocessor in the system should also be considered and the control simplicity should not be ignored. Studies on PMSM have been reviewed considering the problems that may arise in real life, and new researchers will have information about the problems that need to be solved and their solutions with this paper.

**Author Contributions** The concept of the article was determined by OEÖ, MK and SB. The literature research and the preparation of the article were carried out by OEÖ. MK, SB and SE made revisions on the article.

**Funding** The authors did not receive support from any organization for the submitted work.

**Data Availability** Not applicable to this article as no datasets were generated or analyzed during the this study.

**Code Availability** Not applicable to this article as no code were used during the current study.

## Declarations

**Conflict of interest** The authors have no competing interests to declare that are relevant to the content of this article.

## References

1. Wu Y et al (2022) Hierarchical predictive control for electric vehicles with hybrid energy storage system under vehicle-following scenarios. *Energy* 251:123774. <https://doi.org/10.1016/j.energy.2022.123774>
2. Ravi SS, Aziz M (2022) Utilization of electric vehicles for vehicle-to-grid services: progress and perspectives. *Energies* 15(2):589. <https://doi.org/10.3390/en15020589>
3. Bhatt A, Ongsakul W, Madhu MN (2022) Optimal techno-economic feasibility study of net-zero carbon emission microgrid integrating second-life battery energy storage system. *Energy Convers Manag* 266:115825. <https://doi.org/10.1016/j.enconman.2022.115825>
4. Mohanraj D et al (2022) Critical aspects of electric motor drive controllers and mitigation of torque ripple-review. *IEEE*



- Access 10:73635–73674. <https://doi.org/10.1109/ACCESS.2022.3187515>
5. Wang Z et al (2021) Challenges faced by electric vehicle motors and their solutions. *IEEE Access* 9:5228–5249. <https://doi.org/10.1109/ACCESS.2020.3045716>
  6. Agamloh E, von Jouanne A, Yokochi A (2020) An overview of electric machine trends in modern electric vehicles. *Machines* 8(2):20. <https://doi.org/10.3390/machines8020020>
  7. Ding S, Hou Q, Wang H (2022) Disturbance-observer-based second-order sliding mode controller for speed control of PMSM drives. *IEEE Trans Energy Convers.* <https://doi.org/10.1109/TEC.2022.3188630>
  8. Pietrzak P, Wolkiewicz M, Orlowska-Kowalska T (2023) PMSM stator winding fault detection and classification based on bispectrum analysis and convolutional neural network. *IEEE Trans Ind Electron* 70(5):5192–5202. <https://doi.org/10.1109/TIE.2022.3189076>
  9. Shih KJ et al (2022) Machine learning for inter-turn short-circuit fault diagnosis in permanent magnet synchronous motors. *IEEE Trans Magn* 58(8):1–7. <https://doi.org/10.1109/TMAG.2022.3169173>
  10. Zhang Y et al (2021) A rotor position and speed estimation method using an improved linear extended state observer for IPMSM sensorless drives. *IEEE Trans Power Electron* 36(12):14062–14073. <https://doi.org/10.1109/TPEL.2021.3085126>
  11. Tian B et al (2022) Freewheeling current-based sensorless field-oriented control of five-phase permanent magnet synchronous motors under insulated gate bipolar transistor failures of a single phase. *IEEE Trans Ind Electron* 69(1):213–224. <https://doi.org/10.1109/TIE.2021.3053891>
  12. Wu Z et al (2022) Transfer mechanism analysis of injected voltage harmonic and its effect on current harmonic regulation in FOC PMSM. *IEEE Trans Power Electron* 37(1):820–829. <https://doi.org/10.1109/TPEL.2021.3097103>
  13. Kivanc OC, Ozturk SB, Toliyat HA (2022) On-line dead time compensator for PMSM drive based on current observer. *Eng Sci Technol Int J* 25:100987. <https://doi.org/10.1016/j.jestch.2021.04.006>
  14. Nasr A et al (2022) Torque-performance improvement for direct torque-controlled PMSM drives based on duty-ratio regulation. *IEEE Trans Power Electron* 37(1):749–760. <https://doi.org/10.1109/TPEL.2021.3093344>
  15. Li H et al (2021) Feedback linearization based direct torque control for IPMSMs. *IEEE Trans Power Electron* 36(3):3135–3148. <https://doi.org/10.1109/TPEL.2020.3012107>
  16. Bıçak A, Gelen A (2021) Sensorless direct torque control based on seven-level torque hysteresis controller for five-phase IPMSM using a sliding-mode observer. *Eng Sci Technol, Int J* 24(5):1134–1143. <https://doi.org/10.1016/j.jestch.2021.02.004>
  17. Deng W, Li S (2021) Direct torque control of matrix converter-fed PMSM drives using multidimensional switching table for common-mode voltage minimization. *IEEE Trans Power Electron* 36(1):683–690. <https://doi.org/10.1109/TPEL.2020.2998686>
  18. Biyani V et al (2021) Comparative study of different control strategies in permanent magnet synchronous motor drives. In 2021 IEEE 5th international conference on condition assessment techniques in electrical systems (CATCON). pp 275–281. <https://doi.org/10.1109/CATCON52335.2021.9670516>
  19. Niu F et al (2016) Comparative evaluation of direct torque control strategies for permanent magnet synchronous machines. *IEEE Trans Power Electron* 31(2):1408–1424. <https://doi.org/10.1109/TPEL.2015.2421321>
  20. Du Y et al (2022) Self-adapted model predictive current control for five-phase open-end winding pmsm with reduced switching loss. *IEEE Trans Power Electron* 37(9):11007–11018. <https://doi.org/10.1109/TPEL.2022.3167249>
  21. Huang W et al (2022) Open-circuit fault detection in pmsm drives using model predictive control and cost function error. *IEEE Trans Transp Electrification* 8(2):2667–2675. <https://doi.org/10.1109/TTE.2021.3135039>
  22. Wang F et al (2022) Design of model predictive control weighting factors for PMSM using Gaussian distribution-based particle swarm optimization. *IEEE Trans Ind Electron* 69(11):10935–10946. <https://doi.org/10.1109/TIE.2021.3120441>
  23. Gong Z et al (2021) Improved deadbeat predictive current control of permanent magnet synchronous motor using a novel stator current and disturbance observer. *IEEE Access* 9:142815–142826. <https://doi.org/10.1109/ACCESS.2021.3119614>
  24. Dai S et al (2022) Multiple current harmonics suppression for low-inductance PMSM drives with deadbeat predictive current control. *IEEE Trans Ind Electron* 69(10):9817–9826. <https://doi.org/10.1109/TIE.2022.3144577>
  25. Li X et al (2022) Novel deadbeat predictive current control for PMSM with parameter updating scheme. *IEEE J Emerg Sel in Power Electron* 10(2):2065–2074. <https://doi.org/10.1109/JESTPE.2021.3133928>
  26. Ou J, Liu Y, Doppelbauer M (2021) Comparison study of a surface-mounted PM rotor and an interior PM rotor made from amorphous metal of high-speed motors. *IEEE Trans Ind Electron* 68(10):9148–9159. <https://doi.org/10.1109/TIE.2020.3026305>
  27. Koç M (2022) Unified field oriented controlled drive system for all types of PMSMs considering system nonlinearities. *IEEE Access* 10:56773–56784. <https://doi.org/10.1109/ACCESS.2022.3178104>
  28. Özçiflikçi OE, Koç M, Bahçeci S (2021) Maximum torque per ampere strategy in IPM drives for electric vehicles. *El-Cezeri* 8(3):1405–1415. <https://doi.org/10.31202/ecjse.932553>
  29. Preindl M, Bolognani S (2013) Model predictive direct torque control With finite control set for PMSM drive systems, Part 1: maximum torque per ampere operation. *IEEE Trans Ind Inform* 9(4):1912–1921. <https://doi.org/10.1109/TII.2012.2227265>
  30. Li Z, et al (2020) A comprehensive review of state-of-the-art maximum torque per ampere strategies for permanent magnet synchronous motors. In 2020 10th international electric drives production conference (EDPC). <https://doi.org/10.1109/EDPC51184.2020.9388199>
  31. Dianov A et al (2022) Review and classification of MTPA control algorithms for synchronous motors. *IEEE Trans Power Electron* 37(4):3990–4007. <https://doi.org/10.1109/TPEL.2021.3123062>
  32. Preindl M, Bolognani S (2013) Model predictive direct torque control with finite control set for PMSM drive systems, part 2: field weakening operation. *IEEE Trans Ind Inform* 9(2):648–657. <https://doi.org/10.1109/TII.2012.2220353>
  33. Bianchi N et al (2022) A review about flux-weakening operating limits and control techniques for synchronous motor drives. *Energies*. <https://doi.org/10.3390/en15051930>
  34. Sun J, Luo X, Ma X (2018) Realization of maximum torque per ampere control for IPMSM based on inductance segmentation. *IEEE Access* 6:66088–66094. <https://doi.org/10.1109/ACCESS.2018.2876572>
  35. Wang H et al (2020) Maximum torque per ampere (MTPA) control of IPMSM systems based on controller parameters self-modification. *IEEE Trans Veh Technol* 69(3):2613–2620. <https://doi.org/10.1109/TVT.2020.2968133>
  36. Khayamy M, Chaoui H (2018) Current sensorless MTPA operation of interior PMSM drives for vehicular applications. *IEEE Trans Veh Technol* 67(8):6872–6881. <https://doi.org/10.1109/TVT.2018.2823538>
  37. Koç M, Özçiflikçi OE (2022) Precise torque control for interior mounted permanent magnet synchronous motors with recursive least squares algorithm based parameter estimations. *Eng Sci*



- Technol, Int J 34:101087. <https://doi.org/10.1016/j.jestch.2021.101087>
38. Yu H, Wang J, Xin Z (2022) Model predictive control for PMSM based on discrete space vector modulation with RLS parameter identification. *Energies*. <https://doi.org/10.3390/en15114041>
  39. Zhu ZQ, Liang D, Liu K (2021) Online parameter estimation for permanent magnet synchronous machines: an overview. *IEEE Access* 9:59059–59084. <https://doi.org/10.1109/ACCESS.2021.3072959>
  40. Ahn H et al (2020) A review of state-of-the-art techniques for PMSM parameter identification. *J Electr Eng Technol* 15(3):1177–1187. <https://doi.org/10.1007/s42835-020-00398-6>
  41. Sun X et al (2022) Speed sensorless control for IPMSMs using a modified MRAS with gray wolf optimization algorithm. *IEEE Trans Transp Electrif* 8(1):1326–1337. <https://doi.org/10.1109/TTE.2021.3093580>
  42. Ding H, Zou X, Li J (2022) Sensorless control strategy of permanent magnet synchronous motor based on fuzzy sliding mode observer. *IEEE Access* 10:36743–36752. <https://doi.org/10.1109/ACCESS.2022.3164519>
  43. Filho CJV et al (2021) Observers for high-speed sensorless pmsm drives: design methods, tuning challenges and future trends. *IEEE Access* 9:56397–56415. <https://doi.org/10.1109/ACCESS.2021.3072360>
  44. Dhulipati H et al (2021) Torque performance enhancement in consequent pole PMSM based on magnet pole shape optimization for direct-drive EV. *IEEE Trans Magn* 57:1–7. <https://doi.org/10.1109/TMAG.2020.3026581>
  45. Dutta R, Pouramin A, Rahman MF (2021) A novel rotor topology for high-performance fractional slot concentrated winding interior permanent magnet machine. *IEEE Trans Energy Convers* 36(2):658–670. <https://doi.org/10.1109/TEC.2020.3030302>
  46. Chai W et al (2020) Design of a novel low-cost consequent-pole permanent magnet synchronous machine. *IEEE Access* 8:194251–194259. <https://doi.org/10.1109/ACCESS.2020.3032904>
  47. Jeong CL, Kim YK, Hur J (2019) Optimized design of PMSM with hybrid-type permanent magnet for improving performance and reliability. *IEEE Trans Ind Appl* 55(5):4692–4701. <https://doi.org/10.1109/TIA.2019.2924614>
  48. Araz HK, Yılmaz M (2020) Design procedure and implementation of a high-efficiency PMSM with reduced magnetmass and torque-ripple for electric vehicles. *J Faculty Eng Archit Gazi Univ* 35(2):1089–1109
  49. Hu Y et al (2022) Reduction of torque ripple and rotor eddy current losses by closed slots design in a high-speed PMSM for EHA applications. *IEEE Trans Magn* 58(2):1–6. <https://doi.org/10.1109/TMAG.2021.3083664>
  50. Yu Y et al (2023) Analysis of back-EMF harmonics influenced by slot-pole combinations in permanent magnet vernier in-wheel motors. *IEEE Trans Ind Electron* 70(5):4461–4471. <https://doi.org/10.1109/TIE.2022.3189065>
  51. Mendizabal M et al (2021) Optimum slot and pole design for vibration reduction in permanent magnet synchronous motors. *Appl Sci* 11(11):4849. <https://doi.org/10.3390/app11114849>
  52. Huo J et al (2022) Torque ripple compensation with anti-overvoltage for electrolytic capacitor-less PMSM compressor drives. *IEEE J Emerg Sel Top Power Electron* 10(5):6148–6159. <https://doi.org/10.1109/JESTPE.2022.3175897>
  53. Hu M et al (2022) Selective periodic disturbance elimination using extended harmonic state observer for smooth speed control in PMSM drives. *IEEE Trans Power Electron* 37(11):13288–13298. <https://doi.org/10.1109/TPEL.2022.3187125>
  54. Liu J, Li H, Deng Y (2018) Torque ripple minimization of PMSM based on robust ILC via adaptive sliding mode control. *IEEE Trans Power Electron* 33(4):3655–3671. <https://doi.org/10.1109/TPEL.2017.2711098>
  55. Zhang Z et al (2022) Torque ripple suppression for permanent-magnet synchronous motor based on enhanced LADRC strategy. *J Elect Eng Technol* 17:2753–2760. <https://doi.org/10.1007/s42835-022-01164-6>
  56. Xu J et al (2021) Switching-table-based direct torque control of dual three-phase PMSMS with closed-loop current harmonics compensation. *IEEE Trans Power Electron* 36(9):10645–10659. <https://doi.org/10.1109/TPEL.2021.3059973>
  57. Lin X et al (2020) A stator flux observer with phase self-tuning for direct torque control of permanent magnet synchronous motor. *IEEE Trans Power Electron* 35(6):6140–6152. <https://doi.org/10.1109/TPEL.2019.2952668>
  58. Hakami S, Lee KB (2020) Four-level hysteresis-based DTC for torque capability improvement of IPMSM fed by three-level NPC inverter. *Electronics* 9:1558. <https://doi.org/10.3390/electronics9101558>
  59. Wang X et al (2017) Remedial strategies of T-NPC three-level asymmetric six-phase PMSM drives based on SVM-DTC. *IEEE Trans Ind Electron* 64(9):6841–6853. <https://doi.org/10.1109/TIE.2017.2682796>
  60. Petkar SG, Thippiripati VK (2023) A novel duty controlled DTC of a surface pmsm drive with reduced torque and flux ripples. *IEEE Trans Ind Electron* 70(4):3373–3383. <https://doi.org/10.1109/TIE.2022.3181405>
  61. Rehman AU et al (2022) Computationally efficient deadbeat direct torque control considering speed dynamics for a surface-mounted PMSM drive. *IEEE/ASME Trans Mechatron* 27(5):3407–3418. <https://doi.org/10.1109/TMECH.2021.3140077>
  62. Wang X, Wang Z, Xu Z (2019) A hybrid direct torque control scheme for dual three-phase pmsm drives with improved operation performance. *IEEE Trans Power Electron* 34(2):1622–1634. <https://doi.org/10.1109/TPEL.2018.2835454>
  63. Gu X et al (2022) Improved deadbeat predictive control based current harmonic suppression strategy for IPMSM. *Energies*. <https://doi.org/10.3390/en15113943>
  64. Lin X et al (2020) Deadbeat direct torque and flux control for permanent magnet synchronous motor based on stator flux oriented. *IEEE Trans Power Electron* 35(5):5078–5092. <https://doi.org/10.1109/TPEL.2019.2946738>
  65. Yao C et al (2022) ANN optimization of weighting factors using genetic algorithm for model predictive control of PMSM drives. *IEEE Trans Ind Appl* 58(6):7346–7362. <https://doi.org/10.1109/TIA.2022.3190812>
  66. Xu B et al (2022) An improved three-vector-based model predictive current control method for surface-mounted PMSM drives. *IEEE Trans Transp Electrif* 8(4):4418–4430. <https://doi.org/10.1109/TTE.2022.3169515>
  67. Yunfei L, Chengning Z (2019) A comparative experimental analysis of PMSM between deadbeat prediction current control and field-oriented control. *Energy Proc* 158:2488–2493. <https://doi.org/10.1016/j.egypro.2019.01.382>
  68. Körpe UU et al (2022) Modulated model predictive torque control for interior permanent magnet synchronous machines. *El-Cezeri J Sci Eng (ECJSE)* 9(2):777–787. <https://doi.org/10.31202/ecjse.1008121>
  69. Nasr A et al (2022) A low-complexity modulated model predictive torque and flux control strategy for PMSM drives without weighting factor. *IEEE J Emerg Sel Top Power Electron*. <https://doi.org/10.1109/JESTPE.2022.3152652>
  70. Andino J et al (2022) Constrained modulated model predictive control for a three-phase three-level voltage source inverter. *IEEE Access* 10:10673–10687. <https://doi.org/10.1109/ACCESS.2022.3144669>

71. Scheer R et al (2022) A virtual prototyping approach for development of PMSM on real-time platforms: a case study on temperature sensitivity. *Automot Innov* 5(3):285–298. <https://doi.org/10.1007/s42154-022-00186-0>
72. Li J et al (2022) Current sensor fault-tolerant control for five-phase PMSM drives based on third-harmonic space. *IEEE Trans Ind Electron* 69(10):9827–9837. <https://doi.org/10.1109/TIE.2022.3163541>
73. Albatran S, Khalailieh ARA, Allabadi AS (2020) Minimizing total harmonic distortion of a two-level voltage source inverter using optimal third harmonic injection. *IEEE Trans Power Electron* 35(3):3287–3297. <https://doi.org/10.1109/TPEL.2019.2932139>
74. Koc M, Emiroglu S, Tamyürek B (2021) Analysis and simulation of efficiency optimized IPM drives in constant torque region with reduced computational burden. *Turk J Elec Eng Comput Sci* 29:1643–1658. <https://doi.org/10.3906/elk-2005-152>
75. Liao W et al (2021) An enhanced SVPWM strategy based on vector space decomposition for dual three-phase machines fed by two DC-source VSIs. *IEEE Trans Power Electron* 36(8):9312–9321. <https://doi.org/10.1109/TPEL.2021.3052913>
76. Xu J et al (2022) A novel space vector PWM technique with duty cycle optimization through zero vectors for dual three-phase PMSM. *IEEE Trans Energy Convers* 37(4):2271–2284. <https://doi.org/10.1109/TEC.2022.3171705>
77. Liu S et al (2022) Generic carrier-based PWM solution for series-end winding PMSM traction system with adaptive over-modulation scheme. *IEEE Trans Transp Electrification*. <https://doi.org/10.1109/TTE.2022.3193272>
78. Yoo J, Sul SK (2022) Dynamic overmodulation scheme for improved current regulation in PMSM drives. *IEEE Trans Power Electron* 37(6):7132–7144. <https://doi.org/10.1109/TPEL.2022.3140748>
79. Jing R et al (2022) An overmodulation strategy based on voltage vector space division for high-speed surface-mounted PMSM drives. *IEEE Trans Power Electron* 37(12):15370–15381. <https://doi.org/10.1109/TPEL.2022.3195615>
80. Saeed MSR et al (2022) Double-vector-based finite control set model predictive control for five-phase PMSMs with high tracking accuracy and DC-link voltage utilization. *IEEE Trans Power Electron* 37(12):15234–15244. <https://doi.org/10.1109/TPEL.2022.3188578>
81. Wei J et al (2022) The torque ripple optimization of open-winding permanent magnet synchronous motor with direct torque control strategy over a wide bus voltage ratio range. *IEEE Trans Power Electron* 37(6):7156–7168. <https://doi.org/10.1109/TPEL.2022.3146155>
82. Liu T et al (2021) A MTPA control strategy for mono-inverter multi-PMSM system. *IEEE Trans Power Electron* 36(6):7165–7177. <https://doi.org/10.1109/TPEL.2020.3038797>
83. Han Z, Liu J (2021) Comparative analysis of vibration and noise in IPMSM considering the effect of MTPA control algorithms for electric vehicles. *IEEE Trans Power Electron* 36(6):6850–6862. <https://doi.org/10.1109/TPEL.2020.3036402>
84. Li K, Wang Y (2019) Maximum torque per ampere (MTPA) control for IPMSM drives using signal injection and an MTPA control law. *IEEE Trans Ind Inform* 15(10):5588–5598. <https://doi.org/10.1109/TII.2019.2905929>
85. Jin NZ et al (2022) Virtual signal injection maximum torque per ampere control based on inductor identification. *Energies* 15:4851. <https://doi.org/10.3390/en15134851>
86. Sun T et al (2021) Extended virtual signal injection control for MTPA operation of IPMSM drives with online derivative term estimation. *IEEE Trans Power Electron* 36(9):10602–10611. <https://doi.org/10.1109/TPEL.2021.3057629>
87. Mahmud MH, Wu Y, Zhao Y (2020) Extremum seeking-based optimum reference flux searching for direct torque control of interior permanent magnet synchronous motors. *IEEE Trans Transp Electrification* 6(1):41–51. <https://doi.org/10.1109/TTE.2019.2962327>
88. Lee J, Choi JW (2022) MTPA control method for MIDP SPMSM drive system using angle difference controller and P&O algorithm. *IEEE Trans Power Electron* 37(12):15382–15396. <https://doi.org/10.1109/TPEL.2022.3196400>
89. Chen Z et al (2021) An accurate virtual signal injection control for IPMSM with improved torque output and widen speed region. *IEEE Trans Power Electron* 36(2):1941–1953. <https://doi.org/10.1109/TPEL.2020.3010300>
90. Zhou K et al (2019) Field weakening operation control strategies of PMSM based on feedback linearization. *Energies*. <https://doi.org/10.3390/en12234526>
91. Yoo J, Lee J, Sul SK (2021) Analysis of instability in torque control of sensorless PMSM drives in flux weakening region. *IEEE Trans Power Electron* 36(9):10815–10826. <https://doi.org/10.1109/TPEL.2021.3063720>
92. Liu S et al (2022) Improved flux weakening control strategy for five-phase PMSM considering harmonic voltage vectors. *IEEE Trans Power Electron* 37(9):10967–10980. <https://doi.org/10.1109/TPEL.2022.3164047>
93. Yang H, Zhang Y, Shen W (2022) Predictive current control and field-weakening operation of SPMSM drives without motor parameters and DC voltage. *IEEE J Emerg Sel Top Power Electron* 10(5):5635–5646. <https://doi.org/10.1109/JESTPE.2022.3167273>
94. Liu X, Du Y (2022) Torque control of interior permanent magnet synchronous motor based on online parameter identification using sinusoidal current injection. *IEEE Access* 10:40517–40524. <https://doi.org/10.1109/ACCESS.2022.3167041>
95. Su G et al (2022) Multiparameter identification of permanent magnet synchronous motor based on model reference adaptive system & simulated annealing particle swarm optimization algorithm. *Electronics* 11(1):159. <https://doi.org/10.3390/electronics11010159>
96. Yang N et al (2022) A new model-free deadbeat predictive current control for PMSM using parameter-free luenberger disturbance observer. *IEEE J Emerg Sel Top Power Electron*. <https://doi.org/10.1109/JESTPE.2022.3192883>
97. Chen T, Chen B (2022) Nonlinear identification of PMSM rotor magnetic linkages based on an improved extended kalman filter. *J Sens* 2022:9477659. <https://doi.org/10.1155/2022/9477659>
98. Li W et al (2022) Extended Kalman filter based inductance estimation for dual three-phase permanent magnet synchronous motors under the single open-phase fault. *IEEE Trans Energy Convers* 37(2):1134–1144. <https://doi.org/10.1109/TEC.2021.3129283>
99. Shi Y, Sun K, Huang L, Li Y (2012) Online identification of permanent magnet flux based on extended kalman filter for IPMSM drive with position sensorless control. *IEEE Trans Ind Electron* 59(11):4169–4178. <https://doi.org/10.1109/TIE.2011.2168792>
100. Quang NK, Hieu NT, Ha QP (2014) FPGA-based sensorless PMSM speed control using reduced-order extended Kalman filters. *IEEE Trans Ind Electron* 61(12):6574–6582. <https://doi.org/10.1109/TIE.2014.2320215>
101. Liu X, Zhang G, Mei L, Wang D (2016) Speed estimation with parameters identification of PMSM based on MRAS. *J Control, Autom Electr Syst* 27:527–534. <https://doi.org/10.1007/s40313-016-0253-3>

Springer Nature or its licensor (e.g. a society or other partner) holds exclusive rights to this article under a publishing agreement with the author(s) or other rightsholder(s); author self-archiving of the accepted manuscript version of this article is solely governed by the terms of such publishing agreement and applicable law.